inter.noise
HAMBURG 2016

Vibro-acoustic energy flow through spot-welds in Dynamical Energy Analysis

Timo HARTMANN[1], Gang XIE[2], Janis BAJARS[3], David CHAPPELL[4] and Gregor TANNER[5]
[1,5] University of Nottingham, GB
[2] CDH AG, Germany
[3,4] Nottingham Trent University, GB

ABSTRACT

Dynamical Energy Analysis (DEA) in the form of Discrete Flow Mapping (DFM) is a fairly new mesh-based method for numerically modelling structure borne sound transmission in complex structures. A key feature is the possibility to work directly on existing finite element (FE) meshes avoiding time-consuming and costly re-modelling. Furthermore, DFM provides detailed spatial information about the vibrational energy distribution within a complex structure in the mid-to-high frequency range. In this work we will illustrate the method using a car floor structure which consists of a big panel and several rails connected by spot welds modeled in FE through Rigid Body Elements (RBE).

Keywords: Sound, Transmission I-INCE Classification of Subjects Number(s): 76.9, 75.3

1. INTRODUCTION

Simulations of the vibro-acoustic performance of automobiles are routinely carried out in various design stages. To understand the transmission of structure-borne sound in cars, it is necessary to have effective and efficient modelling tools to support the structural design process ideally before a prototype vehicle is built. The major difficulty in modelling structure-borne sound lies in the complex geometry of the car structure. The Finite Element Method (FEM) can describe geometric details of the car structure with sufficient accuracy in the low frequency region, typically below 500 Hz. High frequency analysis using FEM requires extremely fine meshes of the body structure to capture the shorter wavelengths and, at the current time, such analysis poses significant computational challenges.

The impractical computational cost of FEM for a high frequency analysis is perhaps less of a limitation (considering recent advances in CPU power) than the fact that the structural response at high frequencies is very sensitive to small variations in material properties, boundary conditions etc. This will result in considerable scatter in the dynamic characteristics of real vehicles. Therefore, results from the analysis of an FE model become less meaningful at high frequencies and a statistical representation is necessary. The Statistical Energy Analysis (SEA) [1] has been developed to deal with high frequency problems and leads to relatively small and simple models in comparison with FEM. As such SEA has found widespread applications in the automotive and aviation industry, as well as in architectural acoustics. However, SEA is based on a set of often hard to verify assumptions, which effectively require diffuse wave fields and quasi-equilibrium of wave energy within sub-systems. The gap in frequency range between the FEM and SEA is usually referred as the mid-frequency gap, in which neither FEM or SEA provides a satisfactory solution.

[1]email: timo.hartmann@nottingham.ac.uk
[2]email: gang.xie@cdh-ag.com
[3]email: janis.bajars@ntu.ac.uk
[4]email: david.chappell@ntu.ac.uk
[5]email: gregor.tanner@nottingham.ac.uk

The mid-frequency problem has been extensively investigated in recent decades and many different approaches have been proposed. Among them, the hybrid FEM/SEA method [2] has been arguably the most successful and most popular approach and applications of the hybrid method for a full car structure have been reported in [3–5]. The hybrid method requires partitioning the whole structure into deterministic and statistical parts. With academic structures [2, 6], this partitioning procedure is relatively simple and the hybrid method has been demonstrated to give very good predictions of ensemble averages of the mid-frequency response of uncertain structures. However, for real engineering structures such as cars, the separation between the deterministic and statistical parts is not a trivial task. Furthermore, within the statistical parts of the structure there is also the challenge of designing a partition into sub-systems that satisfy the assumptions required for an SEA treatment.

One alternative to SEA is to instead consider the original vibrational wave problem in the high frequency limit, leading to a ray tracing model of the structural vibrations. Tracking rays including multiple reflections on boundaries can become highly computationally intensive, in particular on curved surfaces and including mode conversion at interfaces. As a result, ray tracing has not yet been widely adopted for mechanical engineering problems. Tracking densities of rays propagated by a transfer operator, instead of tracing the rays themselves, leads to a model for the mean energy density which forms the basis of the Dynamical Energy Analysis (DEA) method introduced in [7]. DEA includes SEA as special case via a low order representation of the transfer operator. Higher order implementations enrich the SEA model with information from the underlying ray dynamics, leading to a relaxation of the stringent SEA assumptions. In particular, in DEA we have much more freedom in sub-structuring the total system and variations of the energy density across sub-structures can be modelled [8].

An efficient implementation of DEA on meshes called Discrete Flow Mapping (DFM) has been presented in [8, 9]. In DFM it is possible to compute vibro-acoustic energy densities in complex structures at high frequencies, including multi-modal propagation and curved surfaces. Coupling at material interfaces is described in terms of reflection/transmission matrices. These matrices are obtained by solving the wave equation locally in the coupling region. It is this last property that also allows DFM to be extended as a hybrid method of the form detailed in Ref. [10]. That is, in the deterministic parts of a hybrid model we may apply FEM, or any other full wave simulation method, as we would in a hybrid FEM/SEA approach. Once we have local wave solutions in the deterministic substructures, then we can form reflection/ transmission matrices, see for example [11]. A DFM model in the statistical part of the structure will then couple to these matrices in the same way as the coupling at material interfaces is incorporated in [8]. The main advantage of a hybrid DFM approach is that we do not have any restrictions on the sub-structuring in the statistical region, and we are able to compute a full geometry-dependent solution, and resolve this solution within sub-structures.

In this paper, we apply the DFM method for to modelling a car floor structure including stiffeners and spot-welds. We briefly describe the structure - the car floor structure also considered in [5]. We will then discuss the simulation method - DFM - itself and explain then how it can be extended to include details of the structure. We focus here on the particular problem, namely, that different parts of the FE mesh are coupled together via spot weld models or via so-called *Rigid Body Elements* (RBEs) [12]. Such a treatment - common in FE modelling - needs to be adapted for DFM. In the last section, we present numerical results both for a plate-like car-floor panel not including the stiffeners as well as the full structure and compare with FEM calculations.

2. DESCRIPTION OF THE FLOOR STRUCTURE

A floor structure from a caravan car [5] is considered in this study. The floor structure consists of a floor panel, two longitudinal rails and six transverse rails, as illustrated in Figure 1. The floor panel is connected to the rails through a number of spot-welds and additional reinforcement plates are placed between the floor panel and rails. The structural material is steel, the total mass is 82.3 kilograms. Material properties and dimensions are listed in Table 1. The FE representation of the floor structure containing approximately 340,000 degrees of freedom is obtained from the complete vehicle body model. The floor panel, rails and reinforcements are

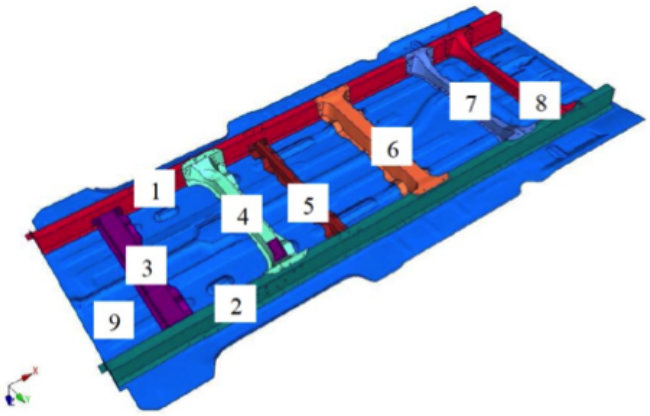

Figure 1. Floor structure, containing rails numbered from 1 to 8 and a panel 9.

modelled using quadrilateral and triangular shell elements. The average element size is 12 mm.

In the following, we will consider this structure in two steps. In a first step, we will only consider the floor panel itself - component 9 (in blue) in Fig. 1. This structure is given here as one mesh consisting of FE shell elements. In a second step, we will then describe the full structure including the rails. Note that, as is typically done in FE treatments, the rails are meshed separately from the panel component 9 and from each other. The rails are physically connected to the panel and to each other in terms of spot welds. They are modelled in terms of RBE elements, see Fig. 2. These elements are well suited for an FE treatment, where interaction can be modelled in terms of vertex (force) connections; however, DFM is based on an energy flow model where flow is measured across interfaces, here the edges of mesh cells. Point connections in terms of RBE elements thus need to be reinterpreted in a DFM setting. In this study here, we propose a way forward, which will make it possible to determine DFM solutions for the full structure. Note that we model the rails as well as the panel using the DFM method.

3. DISCRETE FLOW MAPPING

We will here briefly describe the idea behind DFM, for details see [9]. We will focus here on 2D meshes - an extension of DFM to 3D volume and solid elements is discussed in [13]. We will first consider the case of FE meshes consisting solely of 2D shell and plate elements such as the panel component 9 in Fig. 1 - an extension to modelling connections between different meshes via spot welds and RBE's will be discussed in the next section.

3.1 DFM on 2D surfaces

DFM is a mesh based technique where a transfer operator is used to describe the flow of energy through boundaries of subsystems of the structure; the energy flow is represented in terms of a density of rays ρ, that is, the energy flux through a given surface is given through the density of rays passing through the surface at point s with direction p. Here, s parametrises the surface and p is the direction component tangential to the surface. In what follows, the surfaces is represented by the union of all boundaries of the mesh cells of the FE mesh describing the car floor. The density $\rho(s,p) = \rho(X_s)$, with $X_s = (s,p)$, is transported from one boundary to the next boundary intersection via the boundary integral operator [9]

$$\mathcal{B}[\rho](X'_s) := \int w(X'_s)\delta(X'_s - \phi(X_s))\rho(X_s)\,\mathrm{d}X_s. \tag{1}$$

where $\phi(X_s)$ is the map determining where a ray starting on a boundary segment at point s with direction p_s passes through another boundary segment, and $w(X_s)$ is a factor containing damping and reflec-

Table 1. Floor properties

Material properties	
Young's modulus	$2.1 \times 10^{11}\,\mathrm{N/m^2}$
Poisson ratio	0.3
Density	$7850\,\mathrm{kg/m^3}$
Damping loss factor	0.04 or 0.005
Thickness	
Floor panel	$0.8\,\mathrm{mm}$
Longitudinal rails 1,2	$1.95\,\mathrm{mm}$
Transverse rail 3	$1.35\,\mathrm{mm}$
Transverse rail 4	$1.35\,\mathrm{mm}$
Transverse rail 5	$1.5\,\mathrm{mm}$
Transverse rail 6	$1.5\,\mathrm{mm}$
Transverse rail 7	$1.71\,\mathrm{mm}$
Transverse rail 8	$1.49\,\mathrm{mm}$
Various reinforcements	$2.34\,\mathrm{mm}$
Mass	
Total mass	$82.3\,\mathrm{kg}$
Floor panel	$28.5\,\mathrm{kg}$

tion/transmission coefficients (akin to the coupling loss factors in SEA). As described in [9], the method can be generalised to work efficiently on meshes where the boundary segments are now given by the edges of the mesh cells. Ray densities are transported from a mesh element j to a mesh element i, including reflection when $i = j$. The energy flow is determined as a flow through the edges of the mesh cells, the mapping from one edge to the next is described in terms of straight-line ray-segments with wave-speeds given by the local material parameters and plate thickness. In a next step, the transfer operator (1) is now discretised and represented as a matrix with entries of the form [9]

$$B_{(i,l',m')(j,l,m)} = \frac{2m+1}{2\sqrt{A_l' A_l}} \int_{-c_j^{-1}}^{c_j^{-1}} P_m(p_j) \int_{s_{min}(p_j)}^{s_{max}(p_j)} w_{rt}(p_i') e^{-\eta L(s_j, s_i')} P_{m'}(p_i') ds_j dp_j, \tag{2}$$

where P_m is a scaled Legendre polynomial of order m as detailed in [9], and the energy is propagated along a trajectory through mesh element j with propagation speed c_j. This trajectory starts at position s_j on edge l of element j and is transported to position s_i' on the common edge l' of the boundary of element i. The tangential component of the momentum (or slowness) of the trajectory at s_j is denoted p_j and likewise for p_i' at s_i'. Note, that p_i' and s_i' are uniquely determined by p_j at s_j. Also $L(s_j, s_i')$ is the length of the trajectory from s_j to s_i', η is a (viscous) damping parameter, A_l is the length of edge l from element j, and likewise $A_{l'}$ is the length of edge l' from element i. The integration range in space depends on the momentum, since the admissible range of starting points on edge l that are transported to edge l' must depend on the direction in which the trajectory leaves edge l.

The weight function w_{rt} gives the reflection probability when $i = j$ or the transmission probability otherwise. Note that transmission or reflection at boundaries depends in general on the angle of incidence of the incoming/outgoing ray. DFM incorporates directed transmission through interfaces, in contrast to SEA, which assumes diffusive wave fields in each subsystem. This weight function also governs the mode conversion probabilities in the case of both in-plane and flexural waves, which are derived from wave scattering theory [14]. For modelling the vibrations of the thin shell floor panel we need to consider ray tracing on curved surfaces. Applying thin shell theory in the high frequency limit, as in [15], curved rays follow the

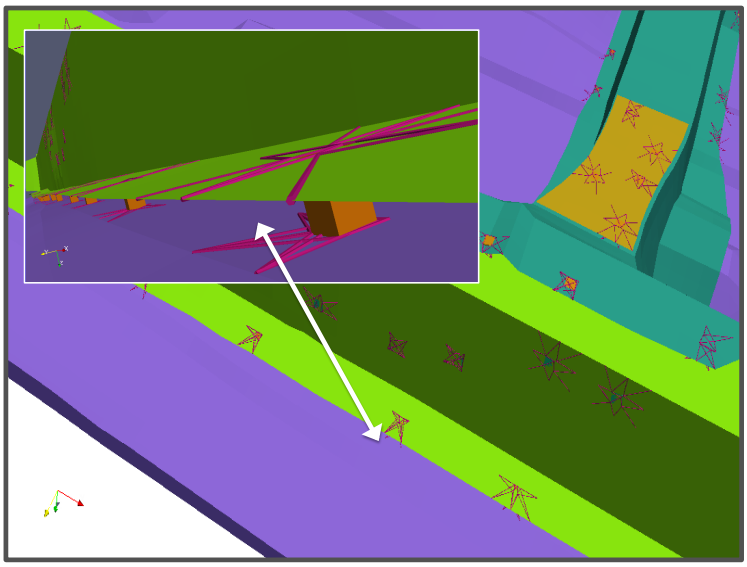

Figure 2: Rail (green) fixed to car floor (purple; component 9 in Fig. 1); the fixtures - spot welds - are modelled with the help of RBEs (red line) and a solid element (orange) mimicking the mass and stiffness properties of the spot weld connection.

geodesics of the surface. This approximation is valid for wavelengths shorter than the radii of curvature of the shell, but larger than the thickness. Mimicking geodesic paths on the corresponding meshed surface, we employ the theory outlined in [16] and [17]. Corrections need to be considered if the radius of curvature is of the order of the wavelength, such as constructing modified ray paths from the governing thin shell theory [15]. However, such corrections require a detailed knowledge of the local curvature and so we will follow a simplified approach here. We treat the meshed structure as a set of plate-like elements and estimate reflection/transmission properties due to the finite angle between mesh elements using the plate-junction theory detailed in [14], see [8, 9] for details.

Once the matrix B has been constructed, the energy density on the boundary phase-space of each element is given by the solution of a linear system of the form

$$(\mathbf{I} - \mathbf{B})\rho = \rho^0, \tag{3}$$

where $\mathbf{I}$ is the identity matrix and $\mathbf{B}$ has entries as defined by equation (2). Here, ρ^0 and ρ are the vectors corresponding to the initial and final boundary densities. Once ρ has been computed, the energy density at any location inside the structure may be computed as a post-processing step, see Ref. [18]. In section 4.1, we compare the results of the above described methodologies for simulating vibrations for the car floor panel, component 9, in Fig. 1.

3.2 Coupled FE meshes

The integral in (2) can be adapted to incorporate further complexity and refinement in a DFM model. The vehicle floor in Fig. 1 contains spot welds fixing the stiff rails to the floor panel. This is modelled in the FE model with the connections shown in Fig. 2, here in terms of a set of RBE's (red lines in Fig. 1) together with solid element modelling extra mass and stiffness of the spot weld. The RBEs describe here constraint conditions and make it possible to transfer forces directly from one mesh to another. Such a set-up can not be used in a DFM treatment which is based on modelling energy flow through surfaces and mesh boundaries. In order to avoid costly remodelling of the structure, we suggest a treatment using the RBEs as coupling elements directly. To describe the energy transfer across spot weld connections as shown in Fig. 2, we keep the form of (1), but introduce coupling between edges connected to the mesh cells next to the spot welds both

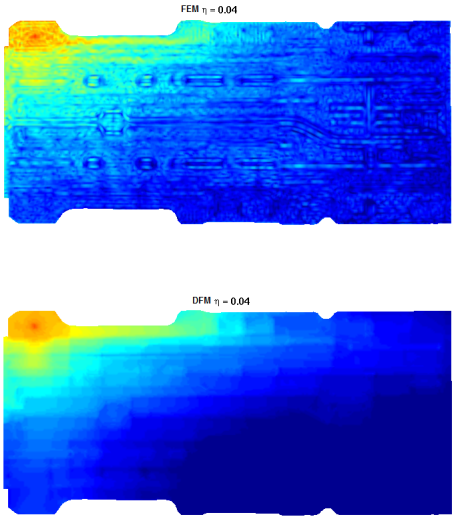

Figure 3: The kinetic energy distribution due to a point source load in the upper left region of the plain floor panel (without rails). The DFM and FEM results are shown with 4% hysteretic damping and the excitation is scaled with the point mobility of the loading so that the input power into the panel from both methods is equal. The results are given on a logarithmic color scale.

in the 'upper' and 'lower' sheet connected by the spot weld. In addition, we calculate the weight function (representing transmission probabilities) via a transfer function.This parameter can be obtained from FE calculations treating single spot welds in isolation or is estimated by analytical calculations. In this treatment, a simplified approach is taken where energy arriving at an edge connected to a spot weld is distributed uniformly among neighbouring edges (ie edges connected by the RBE). In addition, we assume uniform scattering of transmitted rays in all directions. This is an ad-hoc approach, which needs to be refined, for example, local FE models or by the spot weld models used as point connections described in [19]. These point connections transfer circular waves in one part of the structure to circular wave in other parts of the structure. As DFM assumes a plane wave description of the propagation, one has to include an additional step in (2) transforming plane waves to circular waves and back.

4. NUMERICAL RESULTS

In this section we present the simulation results for modelling the car floor structure with the DFM method. We will first discuss results for the bending mode in the floor panel only (without the rails), and compare the results against FEM predictions. In a next step, we will consider the full floor structure in Fig. 1 including the rails coupled to the floor via the spot welds; again both DFM and FEM calculations are considered.

4.1 Comparison of DFM and FEM for a car-floor panel

In order to compare the different numerical approaches we have calculated the spatial kinetic energy distribution originating from a single point excitation on the plain floor panel (shown as component 9 in Fig. 1). The DFM results are compared to one-third octave band frequency-averaged FEM results, with the band average at 2500 Hz. Note that the DFM calculation uses only the band average frequency. The calculation was done for two hysteretic damping loss factors $\eta = 0.04$ and $\eta = 0.005$. The FEM excitation is a unit force load perpendicular to the panel, which primarily excites bending waves. For DFM the force load is converted to an

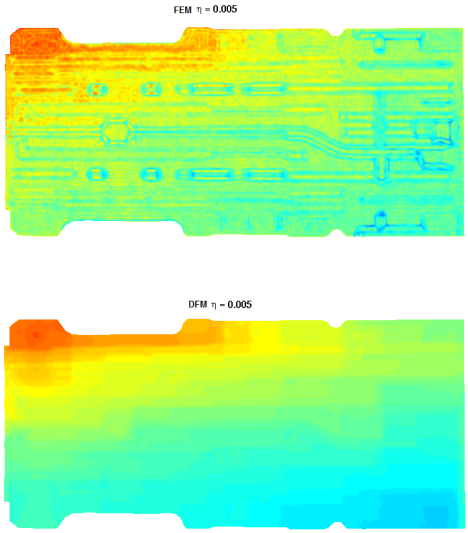

Figure 4: The kinetic energy distribution due to a point source load in the upper left region of the plain floor panel (without the rails). The DFM and FEM results are shown with 0.5% hysteretic damping and the excitation is scaled with the point mobility of the loading so that the input power into the panel from both methods is equal. The results are given on a logarithmic color scale.

injected power flow. This can be done using the Green function of the biharmonic wave equation describing bending waves in an infinite plate. The results for $\nu = 0.04$ are shown in Fig. 3, and the results for the less damped case with $\eta = 0.005$ are shown in Fig. 4. In both cases, the energy distribution predicted by FEM and DFM is very non-uniform and would not be well-captured by an SEA model. In contrast to SEA, DFM gives also the spatial distribution information, which is in close agreement with the FEM results. In particular, we see the directional dependence of the energy flow, which is predominantly in the horizontal direction as plotted. This is caused by several horizontally extended out-of-plane bulges. It is only in the lower right part of the panel, with negligible energy content, that deviations between the FEM and DFM predictions are visible. The results shown in Figs. 3 and 4 also show a good quantitative agreement. In particular, the total kinetic energy given by the DFM prediction is within 6% of the FEM prediction for $\eta = 0.005$, or 12% for $\eta = 0.04$.

Note, that the spatial dependence and directionality of the vibrational energy in the floor panel cannot be obtained from an SEA model. Detailed information about the vibrational energy distribution is, however, very desirable, especially for a component such as the car floor panel stretching across the full vehicle without an obvious way for sub-structuring into smaller SEA subsystems. In the automobile industry, excitations are typically well defined and the associated operational shape is of interest. The results clearly show that modelling bending modes in this panel with DFM captures the full spatial dependence and directionality of the vibrational energy.

4.2 Comparison of DFM and FEM for the full car-floor structure

In a next step, we apply the method described in Sec. 3.2 to perform a DEA calculation for the full car floor model shown in Fig. 1. This includes the coupling of the rails to the floor panel and between different rails via the spot-weld models depicted in Fig. 2. In the DEA calculation, only coupling via RBEs is included and the influence of the solid element is ignored. The results are shown in Fig. 5, here for $\eta = 0.04$ and a frequency band average at 2500 Hz. In contrast to the situation in the previous section, the point loading is

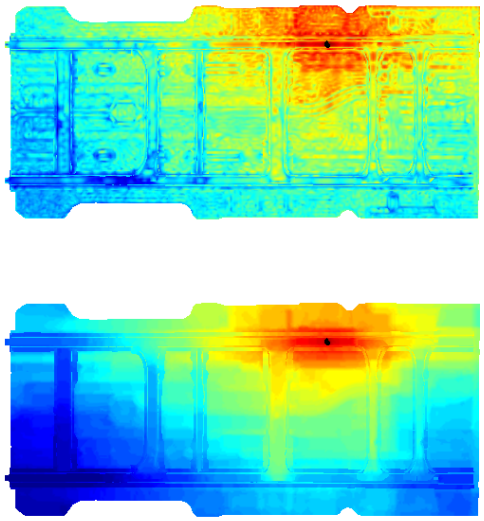

Figure 5: The velocity distribution due to a point source load applied to rail 1 in the full car floor model shown in Fig. 1. The DFM and FEM results are shown with 4% hysteretic damping and the excitation is scaled with the point mobility of the loading so that the input power into the panel from both methods is equal. The results are given on a logarithmic color scale.

now applied on top of a rail, but otherwise equivalent to the situation described in Sec. 4.1. The deviations between the FE result and the DEA result are within 18% when integrated over the total area of the car floor. A detailed analysis shows, that the energy is less pronounced in the DEA calculation compared to the FE calculation when moving away from the source. This suggest that the modelling of the coupling between different components is currently too weak in the DEA model, which calls for a more refined DEA modelling of the RBE connections.

5. CONCLUSIONS

We have tested the DFM method for a car-floor structure at mid- and high- frequencies. The combination of the thin shell floor panel connected to a number of stiffer rails via spot welds posses challenges for a DFM calculations. We have developed a method for treating the coupling of different FE meshes via RBEs in a DFM simulation. The results compare well with (frequency-band averaged) FE calculations both for the floor panel alone and for the full car floor structure. Improvements of the coupling in the DEA set-up needs to be considered.

ACKNOWLEDGEMENTS

Support from the EU (FP7 IAPP grant no. 612237 (MHiVec)) is gratefully acknowledged.

REFERENCES

[1] R.H. Lyon and R.G. DeJong. *Theory and Application of Statistical Energy Analysis*. Butterworth-Heinemann, Boston, 1995.

[2] P.J. Shorter and R.S. Langley. Vibro-acoustic analysis of complex systems. *Journal Sound Vib.*, 288:669–699, 2005.

[3] A. Charpentier, V. Cotoni, and K. Fukui. Using the hybrid fe-sea method to predict structure-borne noise in a car body-in-white. In *Inter-Noise 2006*, Honolulu, Hawaii, USA.

[4] A. Charperntier, S. Sreedhar, and K. Fukui. Efficient model of structure-borne noise in a fully trimmed vehicle from 200hz to 1khz. In *ICSV15 2008*, Daejeon, Korea.

[5] G. Xie, L. Dunne, A. Secgin, and A. Zoghaib. Mid-frequency modelling of a car floor structure with hybrid method and SEA. In *International Symposium on the Computational Modelling and Analysis of Vehicle Body Noise and Vibration*, Sussex, UK, 2012.

[6] V. Cotoni, P.J. Shorter, and R.S. Langley. Numerical and experimental validation of a hybrid finite element-statistical energy analysis method. *J. Acoust. Soc. Amer.*, 122:259–270, 2007.

[7] G. Tanner. Dynamical energy analysis - determining wave energy distributions in vibro-acoustical structures in the high-frequency regime. *J. Sound Vib.*, 320:1023–1038, 2009.

[8] D.J. Chappell, D. Löchel, N. Søndergaard, and G. Tanner. Dynamical energy analysis on mesh grids: A new tool for describing the vibro-acoustic response of complex mechanical structures. *Wave Motion*, 51:589–597, 2014.

[9] D.J. Chappell, G. Tanner, D. Löchel, and N. Søndergaard. Discrete flow mapping: transport of phase space densities on triangulated surfaces. *Proc. R. Soc. A*, 469:20130153, 2013.

[10] D.N. Maksimov and G. Tanner. A hybrid approach for predicting the distribution of vibro-acoustic energy in complex built-up structures. *J. Acoust. Soc. Am.*, 130:1337–1347, 2011.

[11] J.M. Renno and B.R. Mace. Calculation of reflection and transmission coefficients of joints using a hybrid finite element/wave and finite element approach. *J. Sound Vib.*, 332:2149–2164, 2013.

[12] *NX Nastran User's Guide*.

[13] J. Bajars, D.J. Chappell, N. Søndergaard, and G. Tanner. Transport of phase space densities through tetrahedral meshes using discrete flow mapping. *submitted*.

[14] R.S. Langley and K.H. Heron. Elastic wave transmission through plate/beam junctions. *J. Sound Vib.*, 143:241–253, 1990.

[15] A.N. Norris and D.A. Rebinsky. Membrane and flexural waves on thin shells. *ASME J. Vib. Acoust.*, 116:457–467, 1994.

[16] R. Kimmel and J.A. Sethian. Computing geodesic paths on manifolds. In *Proceedings of the National Academy of Sciences of the USA 95*, pages 8431–8435, 1998.

[17] D. Martinez, D.L. Vehlo, and P. C. Carvalho. Computing geodesics on triangular meshes. *Computers & Graphics*, 29:667–675, 2005.

[18] D.J. Chappell and G. Tanner. Solving the stationary Liouville equation via a boundary element method. *J. Comp. Phys.*, 234:487–498, 2013.

[19] R.S. Langley and P.J. Shorter. The wave transmission coefficients and coupling loss factors of point connected structures. *J. Acoust. Soc. Amer.*, 113:1947–1964, 2003.